Electronic Supplementary Material (ESI) for Green Chemistry.

Co-electrolysis of CO_2 and glycerol for the decarbonization of add-value products dihydroxyacetone and formate

Marta Rumayor, Antonio Dominguez-Ramos, Angel Irabien*

SUPPLEMENTARY INFORMATION

1. Benchmark processes

HCOONa: $HCOO^-$ salts are produced in the industry by a direct process based on the reaction of fossil raw materials carbon monoxide (CO) with a base, as sodium hydroxide (NaOH) (1). These raw materials are heated (at temperature of 200°C) under pressure (10 atm) to form sodium formate. According to the Ecoinvent dataset [1], the amount of CO and NaOH entering the process is calculated via stoichiometric equation. The efficiency of the reaction is assumed to be 95%, thus the amount of all the substances entering the process is multiplied by (1/0.95). In the case of CO_2 the unreacted amount is assumed to be treated (flared) and emitted into the air. The unreacted amount of sodium hydroxide is assumed to be emitted to water as sodium, ion (Na-) and hydroxide (OH-) as a part of wastewater. It is assumed that internal wastewater treatment is a part of the activity. Its efficiency is assumed to be 90%, thus only 10% of the unreacted amount of substances which are present in the wastewater are lately released into the environment.

$$NaOH_{(aq)} + CO \rightarrow HCOONa_{(aq.)} \qquad (1)$$

Just as HCOOH, $HCOO^-$ have several uses, e.g., in the pharmaceutical, textile, and leather industries for buffering and regulating of pH, as well as a solid deicer in airfields, enzyme stabilizer in liquid detergents and food preservative, etc.[2] Also, $HCOO^-$ is a building block to produce alcohols, carboxylic acids, monomers, etc.[3] This market is expected to grow in the coming years since both chemicals are promising chemicals for hydrogen storage.

DHA: Because this compound is not found in the Ecoinvent database, its dataset comes from literature.[4,5] Despite the conventional production of DHA involves the biotransformation of pure glycerol in aqueous solution through the free cells of the acetic acid bacteria *Gluconobacter* oxydans, it typically requires reaction times of up to 70 h, with a maximum yield of 40% and leads to a high production cost.[6]. The considered chemocatalytic as well as the biocatalytic inventories are summarized in Table S1. Direct CO2 emissions are produced after the flare stack in the industrial site of the condensed stream after the crystallization, as well as during the full oxidation reaction.

Table S1. Inventories of the chemocatalytic and biocatalytic routes (per kg of pure DHA)

Materials&Energy/Route	Chemocatalytic	Biocatalytic	Unit
Crude glycerol	1.86	1.5	kg
Process water	0.83	10.2	kg
Catalyst	0.002	-	kg
Nutrients	-	0.05	kg
Air	10.91	3.1	m^3
Acetone	0.04	-	kg
Butanol	-	0.06	kg
Direct CO_2	0.45	Not reported	kg
Steam	2.73	44.7	MJ
Cooling water	294	818	kg
Natural gas	1.43	-	MJ
Electricity	1.26	-	MJ
Waste	1.67	11.0	kg
Reference	[4]	[5]	

2. CO2 recycling plant (CO2RP) to produce HCOO- and DHA

In this study, we have improved a previous mathematical model [7] to describe the mass and energy balances on the basis of the reactions shown in Table S2. It was assumed neutral to alkaline conditions [8,9] so formate ($HCOO^-$) is produced in the cathode compartment. The black-box model does not include a transfer model so solubility of CO_2 is assumed very high. The soluble CO_2 that reaches the cathode surface is reduced to $HCOO^-$ and H_2O to hydroxide ions (OH^-)

liberating the stoichiometric amount of H_2, in the presence of the correspondent electrolyte in the cathodic compartment of the ER cell. A combination between a Pt-C anode to produce a limited amount of DHA and the traditional anode DSA-O_2 was used in scenario S3 (Figure S1). According to literature, a carbon supported platinum electrode in a bismuth saturated solution is capable of oxidizing glycerol (GLY) to DHA with 100% selectivity at a carefully chosen potential [10].

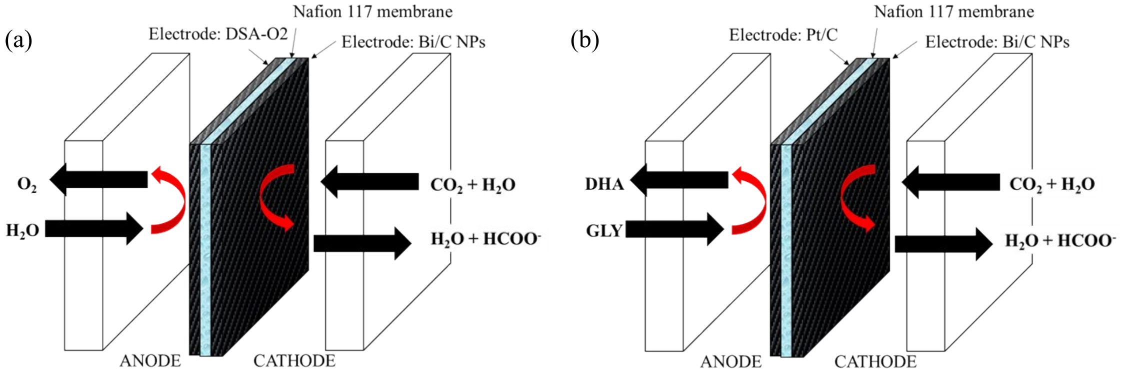

Figure S1. Anodes used in S3: a) traditional DSA-O2 (EOR); b) Pt-C anode (EOG)

When EOR is working on, the formation of oxygen (O_2) is considered as the only reaction taking place in the anodic compartment while when EOR is switch by the EOG anode the formation of the amount of DHA ($C_3H_6O_3$) (limited by its market size) is the unique reaction. As it is known, in an ideal EC reactor, a perfect electrode would lead to a value of 100% for the faradaic current efficiency (FE). This would correspond with the formation of pure $HCOO^-$ in the cathode and pure O_2/DHA in the anode. However, a fraction of the applied current density is deviated to other parallel/parasitic reactions [9], reducing the FE to $HCOO^-$ production. In this study, H_2 evolution reaction (HER) is assumed as the unique parallel reaction in the cathode. The O_2 evolution reaction (OER) when EOR-anode is working and the DHA production when EOR is substituted by the EOG-anode are the only reactions taking place in the anode in each case. Table S3 displays the EC cell performance parameters.

Table S2. Main and side reactions is scenarios in the EC cell

Cathodic Reaction	**Anodic reaction**	
traditional	traditional	EOG alternative
$CO_2 + H_2O + 2e^- \rightarrow HCOO^- + OH^-$	$2OH^- \rightarrow H_2O + 0.5O_2 + 2e^-$	$C_3H_8O_3 + 2OH^- \rightarrow C_3H_6O_3 + 2H_2O + 2e^-$
$2H_2O + 2e^- \rightarrow H_2 + 2\ OH^-$		$2OH^- \rightarrow H_2O + 0.5O_2 + 2e^-$

Table S3. EC cell performance for both anodes

Parameter/Anode	**EOR**	**EOG**
Anode	DSA-O_2	Pt-Bi/C
Cathode	Bi-GDEs	Bi-GDEs
FE_{HCOO-} (cathode) (%)	89.2	89.2
$FE_{O2/DHA}$ (anode) (%)	100 (to O_2)	100 (to DHA)
[HCOO-] M	7.33	7.33
[DHA] M	-	0.04*
Area electrode (cm^2)	10	10
Cell potential (V)	3	1.73
Catholyte	Only humidified CO_2 stream	Only humidified CO_2 stream
Anolyte	1.0 M KOH	0.5 M H_2SO4
Current density, j ($mA \cdot cm^{-2}$)	45	45

*Estimated linearly from the corresponding parameters found in literature [10]

The system boundary of the traditional decarbonization scenario (S2) includes: (i) the capture technology that is based on absorption using MEA (a well-established end-of-pipe technology); (ii) the electrochemical process (using only OER); (ii) purification of formate-based product by distillation; (iii) the optional compression of gas by-products; and (iv) an electric heat unit to supply thermal energy from renewable electricity to the purification and compression steps. The system boundary of the proposed CO2RP as alternative (scenario S3) was expanded to include also: (v) a crude GLY purification step; and (vi) DHA purification (by crystallization technology).

For the cathodic and anodic pumps a simple linear equation was used to calculated the energy per unit of mass of solution pumped [11]. A value of $1.24 \cdot 10^{-4}$ kWh·kg^{-1} is the electricity consumption by the pumps per unit of mass of solution. H_2 produced in the cathode is assumed to be recovered as a by-product (pure). In a similar way, in the anodic compartment, an inlet water stream together with the required chemicals (as GLY in the scenario S3) is injected. Pure O_2 is obtained as by-product of the anodic reaction in S2 which is separated from the water stream by means of a gas/liquid separation unit, and then it can be liquefied and recovered or emitted to the atmosphere. In order to liquefy the pure H_2 and O_2 streams, 10.1 kWh·kg^{-1} and 0.41 kWh·kg^{-1} are the energy needs per unit of mass of H_2 [12] and O_2 [13], respectively. These side products were defined in the study as avoided products from their conventional production processes; therefore, their environmental burden from the reference production processes are avoided.

A purification process in the form of a distillation is required to increase the $HCOO^-$ concentration at the outlet of the cathode compartment to the accepted commercial concentration value at 84% wt. Therefore, cooling and heating are needed. The azeotropic-distillation process was simulated in a previous study carried out by the authors [11]. The simulation considers only presence of water (obtained as a head product) and $HCOO^-$ (obtained as the bottom product) at the required concentration, 84%. According to the simulation, 4.70 MJ·kg^{-1} is the thermal energy consumption per unit of mass of feed stream. Distilled water is recirculated and reinjected to the inlet freshwater stream to the cathode. Then, net water consumption is the difference between water in the inlet stream and water that is recirculated.

In S3 scenario, GLY is the raw material feed to the anode. The system includes a crude GLY purification stage due to crude GLY waste from biodiesel contains some impurities such as methanol, soap, catalysts, salts, matter organic non-glycerol (MONG), and water [14] that have to be removed. The mass and energy balances of crude GLY purification process (Table S4) were found in literature [15].

Table S4. Inventory of GLY purification

Item	Value	Unit

Output		
Glycerol 99.5%	1	ton
Input		
Crude glyc	1.3	ton
Water	0.0521	m^3
Electricity	20	kWh
Heat	5.066	MJ
Sodium hydroxide	1.3	kg
Carbon black	1.5	kg
Compressed air	2	Nm^3

The DHA stream that contains also the unreacted GLY and water is further treated to produce pure DHA at solid state ready to be commercialized. The aqueous DHA stream passes through a first evaporator that removes most part of the water to be recirculated. This was simulated by Aspen Plus software v9 [16] obtaining a value of heat consumption of 0.99 $MJ\cdot kg^{-1}$ (per unit of mass of water in the feed stream). The unreacted GLY is supposed to be perfectly separated and recirculated to the anode compartment of the EC cell consuming. After flashing out water and glycerol, an evaporative crystallization in the presence of acetone, washing and drying stages were modelled on the basis of the simulation of downstream purification of DHA found in literature (Table S5) [4].

Table S5. Inventory of the DHA purification

Item	Value	Unit
Output		
DHA crystallized	1	kg
Input		
Process water	0.83	kg
Air	1.99	m^3
Acetone	0.04	kg
Direct CO_2	0.01	kg
Heat	2.35	MJ
Cooling water	256	kg

Natural Gas	0.04	MJ
Electricity	0.3	MJ
Waste	1.23	kg

In order to check the decarbonization possibilities of the integrated HCOO- and DHA production, their conventional process was taken also as reference. Sodium formate salt production was selected as the reference process for HCOO- [1] and the chemocatalytic process [4] for the DHA production. Note that despite DHA was traditionally produced by a biocatalytic transformation of pure glycerol through the acetic acid bacteria *Gluconobacter oxydans*, which is seen in Table S1 [5], we considered its chemocatalytic process dataset according with literature [4]. The inventory of the production of 1.00 kg of HCOO-+0.47 kg of DHA (as functional unit) by the reference processes (S_{CONV}), by the first decarbonization approach (S2) and by the proposed alternative in the present study for a joint decarbonization (S2) are displayed in Table S6.

Table S6. Material and energy inventories

		Scenarios		
		Traditional	Proposed alternative	
		S1	S2	S3
Valorized products	Unit	$HCOO^-$ DHA	$HCOO^-$ DHA $O_2^{(c)}$ $H_2^{(c)}$	$HCOO^-$ DHA $H_2^{(c)}$ $O_2^{(c)}$
Raw materials				
CO	kg	0.434	-	-
NaOH	kg	0.619	-	-
CO_2	kg	-	0.957	0.957
MEA make-up	kg		0.002	0.002
H_2O	kg	0.455	1.025	0.424
Crude GLY	kg	0.874	0.874	0.631

Nutrients	kg	-	-	-
Catalyst (zeolite)		0.001	-	-
Products and by-products				
$HCOO^-$ [a]	kg	1.000	1.000	1.000
DHA (crystallized)		0.475	0.475	0.475
O_2	kg	-	0. 388	0.335
H_2	kg	-	0. 005	0.009
Direct CO_2 emission	kg	0.247	0.272	0.106
Energy				
Compression H_2&O_2	kWh	-	0.109	0.028
Electricity				
GRID-MIX	kWh	0.581	0.164	-
EC-Cell	kWh	-	3.500	3.182
Pump	kWh	-	$3.78\cdot10^{-4}$	0.012
Compression CO_2	kWh (10^{-3})	-	1.930	1.930
CO_2 capture	kWh	-	1.07	1.07
DHA purification	kWh	-	-	0.04
GLY purification	kWh (x10^{-3})	-	-	9.7
Heat (as steam)	MJ	3.633	1.283	-
Heat[b]				
$HCOO^-$ purification	MJ	-	17.80	17.8
DHA purification	MJ	-	-	103.7
GLY purification	MJ (10^{-3})	-	-	2.46
Water to electric boiler	kg	-	6.140	34.80
Other utilities related with DHA				
Acetone	kg (10^{-2})	1.900	1.900	1.900
Cooling water	kg	121.6	121.6	121.6
Air compressed	m^3	5.127	5.127	0.945
Natural gas	MJ (10^{-2})	67.02	67.02	1.900
Inert waste	kg	0.784	0.784	

Other utilities for GLY purification				
Process water	m^3 (10^{-4})	-	-	25.30
NaOH	kg (10^{-3})	-	-	63.10
Carbon black	kg (10^{-3})	-	-	72.80
Air compressed	m^3 (10^{-4})	-	-	9.700

---

[a] Note that an amount of water of 0.177 kg is not shown in the table as it is considered in the 84% wt. $HCOO^-$ product

[b] Heat (as steam) is supplied by an electric boiler unit. Values of 4.99 kWh and 33.9 kWh are the electricity consumption by this unit to supply the overall heat demand in S_{OER} and S_{EOG}, respectively.

[c] H_2 and O_2 are considered the subproducts of the process

3. Economic assessment

All costs involved in the process scenarios were estimated using a bottom-up approach using a factorial method [17]. Fixed Cash Cost (TFCC) of production represents the initial investment needed to build the plant and it includes the following costs:

(i) Inside the Battery Limits (ISBL) Plant Costs, as representative of the cost of purchasing and installing all the process equipment that integrates the new plant. The costs were estimated based on the factorial Lang method (1)

$$C = F\sum C_e \tag{1}$$

being C the total plant ISBL capital cost; $\sum C_e$ the total delivered cost of major equipment, and F the installation factor, known as Lang Factor (F equal to 4 was considered in this study).

(ii) Offsite Costs (OSBL), as representative of the additional costs that must be made to the site infrastructure to accommodate adding a new plant or increasing the capacity of an existing plant. Offsite investments were estimated as 40% of the ISBL as it is the percentage usually used as an initial estimate if no details of the site are known.

(iii) Engineering Costs, which include the costs of a detailed design and other engineering services required to carry out the project. As a rule of thumb for engineering costs, it can be estimated as 30% of ISBL plus OSBL cost for small projects.

(iv) Contingency Charges stand for the extra costs added into the project budget to allow for variations from the initial cost estimate. A minimum contingency charge of 10% of ISBL plus OSBL cost was used in the present study.

(v) Working Capital is the additional investment above the investment cost to build the plant, to start the plant up and to run it until it starts the earning incomes. Working capital was assumed to be 15% of the fixed capital (ISBL plus OSBL cost).

The Variable Costs of Production (VCP) include the costs of: i) raw materials consumed by the process, ii) utilities, and iii) consumables. These costs were estimated based on the performed mass and energy balances and the material prices.

The Fixed Costs of Production (FCP) are those incurred regardless of the plant operation rate or output. These costs are estimated as a percentage of the operating labour, ISBL and the working capital. Fixed costs included in this work are:

(i) Operating labour— considering a plant operated on a shift-work basis. 4 operators, 3 shift positions and a daily wage and labour cost value of 27.4 € [18].

(ii) Supervision—taken as 25% of the operating labour.

(iii) Direct salary overhead—40% of the operating labour plus the supervision.

(iv) Maintenance, which includes both materials and labour, and is typically estimated as 3% of the ISBL investment.

(v) Property taxes and insurance—typically 1% of the ISBL fixed capital.

(vi) Interest— estimated as 6% of the working capital

The Net Present Value (NPV) is a very well-known indicator for the evaluation of the profitability of the utilization plant from a private investor perspective. The NPV is the sum of the present values of the future cash flows as shown in eq. 2:

$$NPV = \sum_{n=1}^{n=t} \frac{CF_n}{(1+i)^n} - INV \tag{2}$$

being CF_n the net cash flow in the year *n*, *t* the plant life expressed in yr, *INV* the initial investment, which corresponds to the CAPEX, and *i* the interest rate. The NPV is always less than the total future worth of the project because of the discounting of future cash flows [17]. The net cash inflows were calculated based on the purchase price of the products (FA, H_2 and O_2) and their annual produced amount. The interest rate, *i,* is the sum of two terms: i) the market risk premium (MRP), and ii) the risk-free rate (RFR). MRP and RFR ranges in EU for the year 2018 were between 15.8%-5.1% and 5.2%-1.1%, respectively [19]. In this study, an average value of 9% was selected as representative of the *i* for the North West Europe area. Additionally, a sensitivity analysis of the influence of *i* in the profitability of the project, in terms of NPV, were carried out using the highest EU interest rate (Greece, 20.6%) and the lowest EU interest rate (Germany, 6.7%).

Therefore, the revenues of the plant could be calculated as the incomes earned from the sales of the main products and the by-products. The Cash Cost Of Production (CCOP) was determined by the sum of the fixed and variable production costs (minus the by-product revenues). Then, the Total Cost of Production (TCP) was calculated as the sum of the CCOP and the Annual Capital Cost (ACC). The ACC can be evaluated as a function of the discount rate *d* (for the sake of simplicity we assume the same value for the *i* and *d* at 9%), the number of years of the plant *n* and the TFCC according to eq. 3:

$$ACC = \frac{d \cdot (1+d)^n}{(1+d)^n - 1} \cdot TFCC \tag{3}$$

The plant features, cost of equipment and market price of utilities that were considered in the assessment are shown in Table S7.

Table S7. Plant features and unit prices of raw materials, utilities, products, and byproducts

Item	UNIT	Value	Ref
HCOO- production rate	kton·year^{-1}	12	
DHA production to market	kton·year^{-1}	5.7	

Lifetime (Plant)	year	20	
Lifetime cathode+anode	year	4.5	[20]
Lifetime membrane	year	6.84	[20]
Operation time	days·yr^{-1}	350	
Shift per day	h	8	
Hourly labor cost (average EU-27)	€·h^{-1}	27.4	[18]
Discount rate, d		0.09	
Electricity market price (average EU-27)	€·MWh^{-1}	40	[21]
CO_2 price (EU ETS)	€·ton^{-1}	33.87	[22]
H_2 market price	€·kg^{-1}	1.3	[23]
O_2 market price	€·kg^{-1}	0.05	[24]
DHA market price	€·kg^{-1}	2.00	[25]
$HCOO^-$ market price	€·kg^{-1}	0.65	[26]
GLY market price (crude)	€·kg^{-1}	0.02	[27]
NaOH market price	€·kg^{-1}	0.14	[28]
Carbon black market price	€·kg^{-1}	0.93	[20]
Natural gas market price (average EU-27)	€·MJ^{-1}	0.01	[29]
Acetone market price	€·kg^{-1}	0.57	[4]
MEA market price	€·kg^{-1}	1.45	
Compressed air market price	€·m^{-3}	00.0168	[30]
Cooling water	€·kg^{-1}	2.5·10-5	[31]
Water	€·kg^{-1}	0.001	[31]
Capital cost capture	€·ton^{-1}·yr^{-1}	180	[32]
Capital cost electric boiler	M€·MW^{-1}	0.23	[33]
Capital cost crystallizer	k€	39.26	Estimated from [17]
Capital cost distillation	k€	113	Estimated

			from [17]
Capital cost compressor	k€	137	Estimated from [17]
Capital cost pumps	k€	2.9	Estimated from [17]

4. Carbon footprint breakdown results of conventional scenario (S1)

Figure S2 displays the breakdown of the CF overall value (2.8 kg CO2/FU) obtained in the environmental assessment. The influence of the HCOO- and DHA amounts in the functional unit (FU) are shown separately for a better identification. It can be observed that fossil raw materials in $HCOO^-$ production represent the highest contribution. These raw materials are NaOH and CO that are used in the conventional pathway to produce $HCOO^-$. Despite heat and electricity comes from natural gas and grid mix, respectively, and according the Ecoinvent dataset and the literature. Their influence to the overall CF is below 9% (electricity) and % (heat) being raw materials contribution more that 60% to the overall CF value.

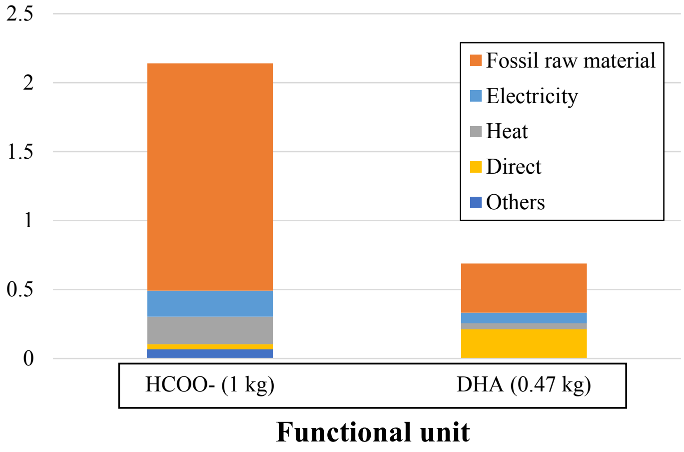

Figure S2. Carbon footprint breakdown of the conventional production of $HCOO^-$ and DHA in S1 scenario

References

[1] Swiss Centre for Life Cycle Inventories, The ecoinvent database Version 7, (2020). http://www.ecoinvent.org (accessed May 3, 2018).

[2] J. Hietala, A. Vouri, J. Pekka, P. Ilkka, W. Reutemann, K. Heinz, Formic Acid, in: Ullmann's Encyclopedia of Industrial Chemistry, Wiley-VCH, Weinheim, Germany, 2000: pp. 1–22. doi:10.1002/14356007.a12_013.

[3] W. Wang, S. Wang, X. Ma, J. Gong, Recent advances in catalytic hydrogenation of carbon dioxide, Chem. Soc. Rev. 40 (2011) 3703–3727. doi:10.1039/C1CS15008A.

[4] G.M. Lari, C. Mondelli, S. Papadokonstantakis, M. Morales, K. Hungerbühler, J. Pérez-Ramírez, Environmental and economic assessment of glycerol oxidation to dihydroxyacetone over technical iron zeolite catalysts, Reaction Chemistry and Engineering. 1 (2016) 106–118. doi:10.1039/c5re00090d.

[5] M. Morales, P.Y. Dapsens, I. Giovinazzo, J. Witte, C. Mondelli, S. Papadokonstantakis, K. Hungerbühler, J. Pérez-Ramírez, Environmental and economic assessment of lactic acid production from glycerol using cascade bio- and chemocatalysis, Energy and Environmental Science. 8 (2015) 558–567. doi:10.1039/c4ee03352c.

[6] R. Ciriminna, A. Fidalgo, L.M. Ilharco, M. Pagliaro, Dihydroxyacetone: An Updated Insight into an Important Bioproduct, ChemistryOpen. 7 (2018) 233–236. doi:10.1002/open.201700201.

[7] M. Rumayor, A. Dominguez-Ramos, P. Perez, A. Irabien, A techno-economic evaluation approach to the electrochemical reduction of CO2 for formic acid manufacture, Journal of CO2 Utilization. 34 (2019) 490–499. doi:10.1016/j.jcou.2019.07.024.

[8] H. Li, C. Oloman, Development of a continuous reactor for the electro-reduction of carbon dioxide to formate – Part 1: Process variables, Journal of Applied Electrochemistry. 36 (2006) 1105–1115. doi:10.1007/s10800-006-9194-z.

[9] C. Oloman, H. Li, Electrochemical processing of carbon dioxide., ChemSusChem. 1

(2008) 385–391. doi:10.1002/cssc.200800015.

[10] Y. Kwon, Y. Birdja, I. Spanos, P. Rodriguez, M.T.M. Koper, Highly selective electro-oxidation of glycerol to dihydroxyacetone on platinum in the presence of bismuth, ACS Catalysis. 2 (2012) 759–764. doi:10.1021/cs200599g.

[11] A. Dominguez-Ramos, B. Singh, X. Zhang, E.G. Hertwich, A. Irabien, Global warming footprint of the electrochemical reduction of carbon dioxide to formate, Journal of Cleaner Production. 104 (2015) 148–155. doi:10.1016/j.jclepro.2013.11.046.

[12] M. Sjardin, K.J. Damen, A.P.C. Faaij, Techno-economic prospects of small-scale membrane reactors in a future hydrogen-fuelled transportation sector, Energy. 31 (2006) 2523–2555. doi:10.1016/J.ENERGY.2005.12.004.

[13] R. Singla, K. Chowdhury, Mitigating an increase of specific power consumption in a cryogenic air separation unit at reduced oxygen production, IOP Conference Series: Materials Science and Engineering. 171 (2017) 012016. doi:10.1088/1757-899X/171/1/012016.

[14] F. Shahidi, Bailey's Industrial Oil and Fat Products, in: & J.W., Sons (Eds.), sixth ed, 2005.

[15] W. Menezes, M.F. Paim, V.G. Maciel, M. Portilho, S. Einloft, M. Seferin, Life cycle assessment of glycerol, by product of the biodiesel production, in: Energy for Sustainability 2013, 2013. http://www2.dem.uc.pt/centerindustrialecology/.

[16] Aspen Technology Inc., ASPEN PLUS v9, (2019). http://home.aspentech.com/.

[17] G. Towler, R. Sinnott, Chemical Engineering Design, Principles, practice, and economics of plant design, 2013.

[18] Eurostat, Wages and labour costs, (2020). http://ec.europa.eu/eurostat/statistics-explained/index.php/Wages_and_labour_costs#Labour_costs (accessed July 12, 2019). (accessed December 1, 2020).

[19] P. Fernandez, V. Pershin, I. Fernández Acín, Market Risk Premium and Risk-Free Rate used for 59 Countries in 2018: A Survey, 2018. doi:10.2139/ssrn.3155709.

[20] M. Rumayor, A. Dominguez-Ramos, A. Irabien, Environmental and economic assessment of the formic acid electrochemical manufacture using carbon dioxide : Influence of the electrode lifetime, Sustainable Production and Consumption. 18 (2019) 72–82. doi:10.1016/j.spc.2018.12.002.

[21] The European Commission, Quarterly Report on European Electricity Markets, 2020.

[22] European Commission, The European Commission's welcome page on the EU ETS, (2015). http://ec.europa.eu/clima/policies/ets/index_en.htm (accessed October 25, 2018).

[23] G. Glenk, S. Reichelstein, Economics of converting renewable power to hydrogen, Nature Energy. 4 (2019) 216–222. doi:10.1038/s41560-019-0326-1.

[24] D. Bellotti, A. Sorce, M. Rivarolo, L. Magistri, Techno-economic analysis for the integration of a power to fuel system with a CCS coal power plant, Journal of CO2 Utilization. 33 (2019) 262–272. doi:10.1016/j.jcou.2019.05.019.

[25] Vass, B. Endrődi, C. Janáky, Coupling electrochemical carbon dioxide conversion with value-added anode processes: An emerging paradigm, Current Opinion in Electrochemistry. 25 (2021) 1–9. doi:10.1016/j.coelec.2020.08.003.

[26] D.J. Drury, Formic acid, in: Kirk-Othmer Encyclopedia of Chemical Technology, John Wiley & Sons, Inc., 2013: pp. 1–9. doi:https://doi.org/10.1002/0471238961.0615181304182118.a01.pub2.

[27] L.R. Kumar, R. Kaur, R.D. Tyagi, P. Drogui, Identifying economical route for crude glycerol valorization: Biodiesel versus polyhydroxy-butyrate (PHB), Bioresource Technology. 323 (2021) 124565. doi:10.1016/j.biortech.2020.124565.

[28] A.S. Agarwal, Y. Zhai, D. Hill, N. Sridhar, The electrochemical reduction of carbon dioxide to formate/formic acid: Engineering and economic feasibility, ChemSusChem. 4

(2011) 1301–1310. doi:10.1002/cssc.201100220.

[29] Eurostat, Natural gas prices for household consumers, first half 2020, (2021). https://ec.europa.eu/eurostat/statistics-explained/index.php/Natural_gas_price_statistics#Natural_gas_prices_for_non-household_consumers (accessed March 2, 2021).

[30] C.A. Solutions, Compressed Air Solutions, (2020). https://www.compressedairsolutions.co.uk/knowledge-bank/cost-of-compressed-air/%0A (accessed March 2, 2021).

[31] M. Pérez-Fortes, E. Tzimas, Techno-economic and environmental evaluation of CO2 utilisation for fuel production - Synthesis of methanol and formic acid, 2016. doi:10.2790/31552.

[32] T. Fleiter, A. Herbst, M. Rehfeldt, M. Arens, Industrial Innovation: Pathways to deep decarbonisation of Industry. Part 2: Scenario analysis and pathways to deep decarbonisation, (2019) 95.

[33] T. Fleiter, J. Steinbach, M. Ragwitz, A.H. Marlene Arens, Ali Aydemir, Rainer Elsland, Tobias Fleiter, Clemens Frassine, S. Hirzel, M. Krail, M. Ragwitz, M. Rehfeldt, M. Reuter, J. Steinbach, J. Dengler, B. Köhler, A. Dinkel, P. Bonato, N. Azam, D. Kalz, F.A. Toro, C. Gollmer, F. Reitze, M. Schön, E. Jochem, F. Tuillé, GaëtanFovez, D. Lescot, M. Hartner, L. Kranzl, A. Müller, S. Fothuber, A. Hiesl, M. Hummel, G. Resch, E. Aichinger, S. Fritz, L. Liebmann, A. Toleikytė, U. Reiter, G. Catenazzi, M. Jakob, C. Naegeli, Mapping and analyses of the current and future (2020 - 2030) heating/cooling fuel deployment (fossil/renewables), 2016.